Autophagy 6:8, 1078-1089; November 16, 2010; © 2010 Landes Bioscience

Suppression of autophagy permits successful enzyme replacement therapy in a lysosomal storage disorder—murine Pompe disease

Nina Raben,[1,*] Cynthia Schreiner,[1,†] Rebecca Baum,[1,†] Shoichi Takikita,[1] Sengen Xu,[1] Tao Xie,[1] Rachel Myerowitz,[1] Masaaki Komatsu,[2] Jack H. Van Der Meulen,[3] Kanneboyina Nagaraju,[3] Evelyn Ralston[4] and Paul H. Plotz[1]

[1]Arthritis and Rheumatism Branch and [4]Light Imaging Section; Office of Science & Technology; National Institute of Arthritis and Musculoskeletal and Skin Diseases; National Institutes of Health; Bethesda, MD USA; [2]Tokyo Metropolitan Institute of Medical Science; Tokyo Japan; [3]Research Center for Genetic Medicine; Children's National Medical Center; Washington, DC USA

[†]These authors contributed equally to this work.

Key words: Pompe disease, lysosomal glycogen storage, myopathy, Atg7, enzyme replacement therapy

Abbreviations: GAA, acid alpha-glucosidase; ERT, enzyme replacement therapy; GSK, glycogen synthase kinase; GS, glycogen synthase; LAMP-2, lysosomal-associated membrane protein 2; LC3, microtubule-associated protein 1 light chain 3

Autophagy, an intracellular system for delivering portions of cytoplasm and damaged organelles to lysosomes for degradation/recycling, plays a role in many physiological processes and is disturbed in many diseases. We recently provided evidence for the role of autophagy in Pompe disease, a lysosomal storage disorder in which acid alpha-glucosidase, the enzyme involved in the breakdown of glycogen, is deficient or absent. Clinically the disease manifests as a cardiac and skeletal muscle myopathy. The current enzyme replacement therapy (ERT) clears lysosomal glycogen effectively from the heart but less so from skeletal muscle. In our Pompe model, the poor muscle response to therapy is associated with the presence of pools of autophagic debris. To clear the fibers of the autophagic debris, we have generated a Pompe model in which an autophagy gene, *Atg7*, is inactivated in muscle. Suppression of autophagy alone reduced the glycogen level by 50–60%. Following ERT, muscle glycogen was reduced to normal levels, an outcome not observed in Pompe mice with genetically intact autophagy. The suppression of autophagy, which has proven successful in the Pompe model, is a novel therapeutic approach that may be useful in other diseases with disturbed autophagy.

Introduction

The lysosomal glycogen storage disorder, Pompe disease, is caused by deficiency of acid alpha-glucosidase (GAA), the sole hydrolase responsible for the breakdown of glycogen to glucose in the acidic milieu of the lysosome. The lack or insufficient activity of GAA results in accumulation of lysosomal glycogen that primarily affects cardiac and skeletal muscles.[1] In infants the disease manifests as a rapidly progressive skeletal myopathy and cardiomyopathy with death occurring within the first year of life from cardiac failure.[2] In milder late-onset forms cardiac muscle is spared, but a slowly progressive muscular disorder eventually leads to death from respiratory failure.[3]

Enzyme replacement therapy (ERT) with recombinant human GAA (rhGAA; Myozyme®, alglucosidase alfa, Genzyme Corp., Framingham, MA) is the first approved therapy for this devastating disorder. It has proven to be very efficient in rescuing the cardiac abnormalities and thus significantly extending the life span of infants, but its effect in skeletal muscle falls short of expectations.

It is not clear why skeletal muscle is such a difficult target for ERT. The sheer mass of skeletal muscle, the diversion of the administered enzyme to the liver and the low density of the mannose-6-phosphate receptor (which is responsible for the endocytosis of the rhGAA) on muscle cells contribute to, but do not fully explain, the limited benefit of therapy. In fact, both in humans and in GAA$^{-/-}$ mice glycogen accumulation persists even when the enzyme activity reaches normal or near normal levels in muscle.[4-6] This suggests that some intrinsic properties of muscle cells play a role. We have found that muscle fibers in the GAA$^{-/-}$ mice and in patients with the disease contain large pools of autophagic debris in addition to the enlarged glycogen-filled lysosomes.[7,8] In the GAA$^{-/-}$ mice, this autophagic buildup is seen in therapy-resistant fast muscles but not in slow muscles which respond well to therapy. We have also shown that a significant portion of the therapeutic enzyme is diverted to the area of autophagic accumulation in GAA$^{-/-}$ mice.[7]

*Correspondence to: Nina Raben; Email: rabenn@mail.nih.gov
Submitted: 05/25/10; Revised: 08/16/10; Accepted: 08/20/10
Previously published online: www.landesbioscience.com/journals/autophagy/article/13378
DOI: 10.4161/auto.6.8.13378

Macroautophagy (referred to as autophagy), the major lysosome-dependent catabolic pathway, is required to generate nutrients and energy during starvation and to perform homeostatic functions such as clearance of toxic misfolded proteins or damaged organelles.[9-11] The autophagic process involves sequestration of a portion of the cytoplasm by double-membrane autophagosomes, which deliver their contents to lysosomes for degradation. Dysfunctional autophagy has been found in many lysosomal storage disorders[12,13] as well as in other major disease groups, such as neurodegenerative diseases, malignancy, inflammatory diseases, etc.[14] The attempt to modulate autophagy by upregulation (in neurodegenerative diseases) or by downregulation (in drug-resistant cancer cells) has led to some promising results.[15,16]

In light of our findings of the association between autophagic buildup and resistance to therapy in Pompe disease, it seemed intuitive that regulation of autophagy might offer an alternative therapy for this disorder. The aim would be to rid muscle cells of the autophagic accumulation and, in addition, possibly reduce the lysosomal glycogen load since autophagy is a presumed mechanism of glycogen trafficking to lysosomes.[17,18]

We previously reported the generation of a GAA$^{-/-}$ model in which a key autophagic gene, *Atg*5, was selectively inactivated in skeletal muscle (AD-GAA KO, which we now refer to as HSAcre:Atg5$^{F/F}$:GAA$^{-/-}$,[19]). Suppression of autophagy in muscle of the GAA$^{-/-}$ mice, indeed, prevented the autophagic buildup, but exacerbated the clinical phenotype of the knockout mice despite somewhat diminished muscle glycogen levels. To verify whether this outcome resulted from the suppression of autophagy alone and not from genetic manipulations or the additional, autophagy-independent role of Atg5 [shown in tumor cells[20]], we made another muscle-specific autophagy-deficient GAA$^{-/-}$ strain by inactivating a different critical autophagic gene, *Atg*7. Furthermore, we chose to limit the suppression of *Atg*7 to the muscles that are affected by the autophagic buildup, namely, fast muscles. Here we demonstrate that suppression of *Atg*7 alone resulted in a substantial reduction of glycogen accumulation in the GAA$^{-/-}$ mice and remarkably, a combination of ERT with the suppression of *Atg*7 led to normalization of glycogen levels. These results prompted us to re-examine the HSAcre:Atg5$^{F/F}$:GAA$^{-/-}$ model and to evaluate the effect of ERT in this previously described strain. We now show that the therapy is successful in both strains despite the phenotypic and biochemical differences between them. Thus, the enhanced correction of muscle glycogen storage by suppression of autophagy suggests a new therapeutic approach for this and possibly other diseases with disturbed autophagy. Further, we provide evidence that glycogen synthase kinase 3β (GSK-3β; a protein involved in glycogen metabolism) is activated and may contribute to the upregulation of autophagy in GAA$^{-/-}$ muscle cells.

Results

Characteristics of the MLCcre:Atg7$^{F/F}$:GAA$^{-/-}$ strain. We have generated GAA$^{-/-}$ mice in which a large segment of the *Atg*7 gene is excised in fast muscle fibers by Cre recombinase; these mice are referred to as MLCcre:Atg7$^{F/F}$:GAA$^{-/-}$. We have also made a control MLCcre:Atg7$^{F/F}$:WT strain in which *Atg*7 is excised in fast muscle fibers of WT mice.

Consistent with our previous data,[19] autophagy is upregulated in muscle of the GAA$^{-/-}$ mice as shown by an increase in both cytosolic LC3-I and autophagosomal membrane-bound LC3-II (**Fig. 1A**). As expected, in the MLCcre:Atg7$^{F/F}$:GAA$^{-/-}$ mice autophagy was considerably suppressed in fast (gastrocnemius, **Fig. 1A**) but less so in slow (soleus, **Fig. 1B**) muscles as indicated by the levels of LC3-II. The suppression of autophagy in fast muscle is further supported by the increase in the level of p62 protein (**Fig. 1C**). The degree of the suppression of autophagy in fast muscles differs in young and old mice, as shown by a progressive decline with age in the levels of LC3-II and Atg7 (**Fig. 1A and Suppl. Fig. 1**). Small clusters of double-membrane vesicles containing undigested cytoplasmic material and possibly glycogen were detected by electron microscopy (**Fig. 2**), but autophagic buildup, which is so prominent in GAA$^{-/-}$ muscle, was not observed in fibers from MLCcre:Atg7$^{F/F}$:GAA$^{-/-}$ mice of any age (**Fig. 1D and Suppl. Video 1**).

Expansion of lysosomes, a hallmark of Pompe disease, persists in muscle fibers from MLCcre:Atg7$^{F/F}$:GAA$^{-/-}$ mice, but the lysosomes in the majority of the fibers are smaller (5-6 μm) than those in the GAA$^{-/-}$ mice (12–15 μm) (**Fig. 1C**). Furthermore, the fibers from MLCcre:Atg7$^{F/F}$:GAA$^{-/-}$ contain a large number of normal-looking, dot-like LAMP-1-positive lysosomes which appear to maintain their acidic pH (**Suppl. Fig. 2A**). Other prominent features of these autophagy-deficient fibers are clustering of lysosomes in the core of fibers (**Suppl. Fig. 2B**) and an age-dependent accumulation of ubiquitinated (Ub) proteins (**Suppl. Fig. 2C–E**).

The most striking finding in MLCcre:Atg7$^{F/F}$:GAA$^{-/-}$ mice, however, is a ~60% reduction in the level of glycogen accumulation in fast muscle compared to that in the GAA$^{-/-}$ mice, suggesting that the suppression of autophagy serves as substrate reduction therapy (**Table 1 and Suppl. Table 1**). The reduced glycogen level is detected in fast but not in cardiac (**Table 1**) or slow muscles (**Suppl. Table 1**), indicating that suppression of autophagy, rather than differences in glycogen metabolism in the two strains, is responsible. Clinically, the MLCcre:Atg7$^{F/F}$:GAA$^{-/-}$ mice are no different from the GAA$^{-/-}$,[21] in terms of muscle wasting, kyphosis and life span.

The absence of autophagic buildup, a significantly reduced glycogen load and the lack of additional clinical manifestations made the MLCcre:Atg7$^{F/F}$:GAA$^{-/-}$ model a promising candidate for enzyme replacement therapy.

Enzyme replacement therapy. Suppression of autophagy combined with ERT resulted in a ~90% decrease of glycogen in fast muscles from MLCcre:Atg7$^{F/F}$:GAA$^{-/-}$ mice when compared to the levels in untreated GAA$^{-/-}$ mice (**Fig. 3A and Table 1**). This glycogen clearance was also shown by PAS staining of muscle biopsies (**Fig. 3B**) and by immunostaining of single fibers for a lysosomal (LAMP-1) marker (**Fig. 3C**). In contrast, ERT-treated GAA$^{-/-}$ mice with genetically intact autophagy had only a ~30% reduction in fast muscles (**Fig. 3A and Table 1**). Furthermore, the autophagic buildup persisted in ERT-treated GAA$^{-/-}$ muscle, as shown by immunostaining of single fibers for an autophagosomal

marker, LC3 (**Fig. 3C and Suppl. Video 2**). As expected, in both strains ERT cleared glycogen from cardiac muscle very efficiently (**Table 1**).

We also tested ERT in another, previously described muscle-specific, autophagy-deficient Pompe model with a higher level of glycogen accumulation.[19] In this model, HSAcre:Atg5$^{F/F}$:GAA$^{-/-}$, the *Atg*5 gene was excised by Cre recombinase driven by the human skeletal actin promoter. Unlike in the MLCcre:Atg7$^{F/F}$:GAA$^{-/-}$ strain, glycogen levels in HSAcre:Atg5$^{F/F}$:GAA$^{-/-}$ mice were insignificantly reduced by only ~20% compared to the GAA$^{-/-}$ (4.0 ± 2.6% wet weight and 5.0 ± 2.8% for HSAcre:Atg5$^{F/F}$:GAA$^{-/-}$ and GAA$^{-/-}$ respectively).[19] With the additional samples the difference (~29%) reached statistical significance, but the glycogen levels still remained much higher than in MLCcre:Atg7$^{F/F}$:GAA$^{-/-}$ mice (**Fig. 3A, Table 1 and Suppl. Table 1**).

Despite the higher level of glycogen, the effect of ERT in HSAcre:Atg5$^{F/F}$:GAA$^{-/-}$ was equally impressive—a complete removal of glycogen was observed (**Fig. 3A and Table 1**). These data were supported by PAS staining of muscle biopsies (**Suppl. Fig. 3**) and by immunostaining of fibers for LC3 and LAMP-1 (shown for MLCcre:Atg7$^{F/F}$:GAA$^{-/-}$ in **Fig. 3C**). Thus, it is the suppression of autophagy rather than the initial level of glycogen accumulation that has an effect on therapy.

We next examined the functionality of the lysosomes in ERT-treated mice by analyzing the level of Ub-proteins. A number of transmembrane proteins and receptors are ubiquitinated and delivered via the endocytic pathway to the lysosomes for degradation.[22,23] Another pool is delivered to the lysosomes via constitutive autophagy.[24-26] Both pools contribute to the accumulation of Ub-proteins in fast GAA$^{-/-}$ fibers,[19] as well as in cells from patients with different lysosomal storage diseases.[27] We observed no appreciable reduction of Ub-proteins in ERT-treated GAA$^{-/-}$ mice (**Fig. 4A**). In contrast, ERT treatment in autophagy-deficient GAA$^{-/-}$ strains resulted in a decrease in the amount of Ub-proteins in both soluble and nonsoluble fractions as shown by western blotting (**Fig. 4B**) and by immunostaining of myofibers (**Fig. 4C**). These data suggest that the lysosomal function in muscles from treated autophagy-deficient GAA$^{-/-}$ mice is largely restored. Thus, the suppression of autophagy in skeletal muscle greatly facilitates the effect of ERT, resulting in an outcome which has not been observed in Pompe mice with genetically intact autophagy.

The functional effect of ERT, however, as assessed by the force of the EDL muscle from treated and untreated autophagy-deficient GAA$^{-/-}$ mice, was not measurable because at the age of these animals (4 months) even untreated GAA$^{-/-}$ mice show no significant difference in the specific isometric tetanic force when compared to the WT (**Suppl. Table 2**).

Although successful reversal of lysosomal pathology is achieved in MLCcre:Atg7$^{F/F}$:GAA$^{-/-}$ mice by ERT, it should be remembered that these animals remain autophagy-deficient in skeletal muscle. Consistent with the previously published data,[28] suppression of autophagy in the control MLCcre:Atg7$^{F/F}$:WT or HSAcre:Atg5$^{F/F}$:WT mice resulted in accumulation of Ub-proteins; this accumulation, however, was modest when compared to that in the GAA$^{-/-}$ (**Fig. 4B**). No weight loss was recorded in 4-month-old MLCcre:Atg7$^{F/F}$:WT animals [21.1 ± 1.0 g (n = 11) and 21.2 ± 2.3 g (n = 7) in WT and MLCcre:Atg7$^{F/F}$:WT respectively] and no major clinical abnormalities were noted in these mice during an observation period of up to two years. These autophagy-deficient mice show muscle atrophy, as evidenced by a tendency toward a reduction in cross-sectional area of EDL muscle (**Suppl. Table 2**) and by a reduced diameter of single psoas (fast) fibers (**Suppl. Table 3**). The maximum Ca^{+2}-activated isometric force generated by single psoas fibers were

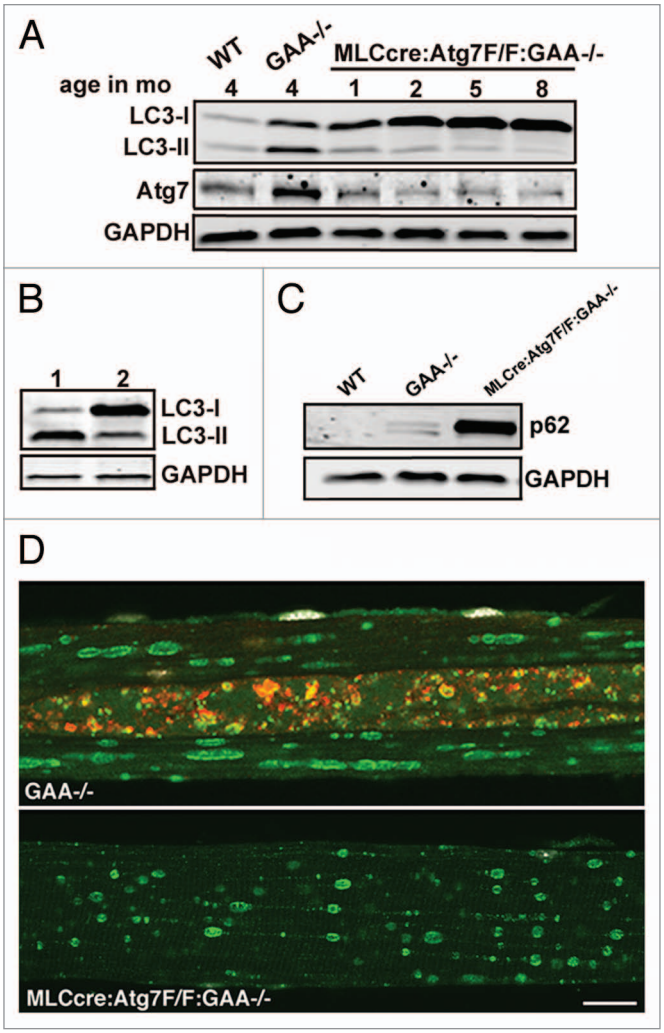

Figure 1. Autophagy is suppressed in fast muscles from MLCcre:Atg7$^{F/F}$:GAA$^{-/-}$ mice. (A) Western blot of protein lysates from gastrocnemius (fast) muscles derived from WT, GAA$^{-/-}$ and MLCcre:Atg7$^{F/F}$:GAA$^{-/-}$ mice with LC3 (top part) or with Atg7 antibody (middle part) (n = 10 for each age group). (B) Western blot of lysates from soleus (slow) muscle derived from 6-month-old GAA$^{-/-}$ (lane 1) and MLCcre:Atg7$^{F/F}$:GAA$^{-/-}$ (lane 2) mice with LC3. LC3-II is consistently present in slow muscle from MLCcre:Atg7$^{F/F}$:GAA$^{-/-}$ mice although the levels are lower than in GAA$^{-/-}$ mice. The data are representative of at least five independent experiments. GAPDH serves as a loading control. (C) Western blot of protein lysates from gastrocnemius (fast) muscles derived from WT, GAA$^{-/-}$ and MLCcre:Atg7$^{F/F}$:GAA$^{-/-}$ mice with p62 antibody (n = 10 for each age group). Muscle samples were taken from 3–4.5 month-old mice. (D) Immunostaining of single psoas (fast) fibers stained for LAMP-1 (green) and LC3 (red). Muscle samples were taken from 4-month-old mice. Bar: 20 microns.

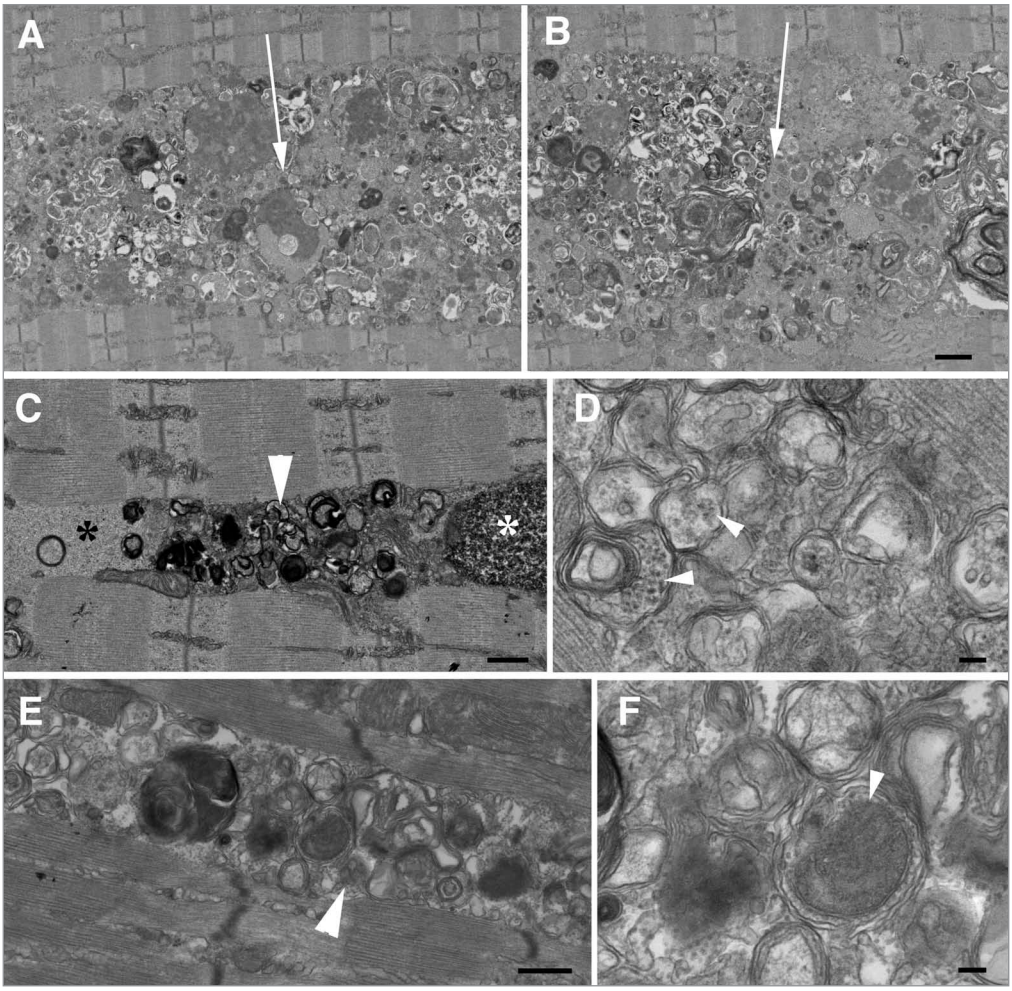

Figure 2. Electron microscopy confirms the disappearance of autophagic buildup in fast muscles of MLCcre:Atg7$^{F/F}$:GAA$^{-/-}$ mice and provides evidence for the presence of residual autophagy-related vesicles. (A and B) Two non-overlapping images of a single continuous area of autophagic accumulation in the psoas muscle of a 10 month-old GAA$^{-/-}$ mouse illustrate the impressive size of such areas, which were not encountered in muscle from age-matched MLCcre:Atg7$^{F/F}$:GAA$^{-/-}$ mice (C–E). However, limited accumulations of nonlysosomal vesicular material are seen in the psoas muscle of MLCcre:Atg7$^{F/F}$:GAA$^{-/-}$ mice (arrowheads in C and E). Vesicles are often found adjacent to glycogen-laden lysosomes (C, white asterisk) and to accumulations of Ub-proteins (C, black asterisk). (D) shows a detailed view of multi-membrane vesicles, some of which (D, small arrowheads) may contain glycogen. (F) shows a higher magnification image of the area in (E); one of the vesicles (small arrowheads) resembles a pre-autophagosome membrane cup. Bars: (A and B): 1 micron; (C and E): 500 nanometers; (D and F): 100 nanometers.

lower than in the WT but higher than in the GAA$^{-/-}$ (**Suppl. Table 3**). In addition, the overall muscle strength, as measured by a grip strength test, of the autophagy-deficient mice was lower than the WT (**Suppl. Table 4**).

Possible triggers of autophagy in fast muscle of GAA$^{-/-}$ mice. We have previously shown that autophagy is upregulated in Pompe muscle.[19] We now add two additional pieces of information supporting the upregulation of autophagy: Beclin 1, a protein known to be activated during autophagy induction,[29] and the Atg7 protein are increased in GAA$^{-/-}$ fast muscle (**Figs. 1A and 5A**).

Unraveling the mechanisms of autophagic disturbance in skeletal muscle under pathological conditions is a daunting task, particularly because skeletal muscle is a peculiar tissue in terms of how it responds to the classic inducers of autophagy—starvation and an mTOR inhibitor, rapamycin. Unlike cardiac muscle, WT fast muscle showed no appreciable increase in the amount of LC3-II following 24 or 48 hours of starvation (**Suppl. Fig. 4A and B**). This outcome was unexpected because it had been previously shown that starvation did result in conversion of LC3-I to LC3-II in muscle.[30] The discrepancy may be attributed to the differences in the kind of muscles used (we consistently use only the white part of the gastrocnemius muscle), the genetic background and the age of the animals. For starvation experiments, we routinely use 4–5 month-old animals; in young, ~1 month old mice, we, too, see a mild response to starvation but the results are inconsistent (not shown).

Rapamycin also does not induce autophagy in WT skeletal muscle as shown by us (**Suppl. Fig. 4C**) and others.[31] Similar to the effect of rapamycin in the WT, no increase in LC3-II was detected in muscle from GAA$^{-/-}$ mice although mTOR activity was suppressed by the drug, as evidenced by a decrease in the

Table 1. The effect of ERT on glycogen levels (μg glucose/hr/mg protein) in GAA$^{-/-}$ and autophagy-deficient GAA$^{-/-}$ strains

Genotype	Tissue	Untreated	Treated	% Reduction*
GAA$^{-/-}$	Gastroc	71.9 ± 22.7 (n = 29)	52.5 ± 22.7 (n = 14)	29
	Quad	75.7 ± 24.8 (n = 31)	54.5 ± 29.6 (n = 12)	30
	Heart	197.4 ± 41.7 (n = 13)	0.6 ± 1.2 (n = 12)	100
MLCcre:Atg7$^{F/F}$:GAA$^{-/-}$	Gastroc	25.0 ± 13.4 (n = 18)	8.6 ± 8.9 (n = 9)	94
	Quad	35.0 ± 18.4 (n = 17)	13.7 ± 10 (n = 9)	87
	Heart	199.2 ± 79.1 (n = 13)	0.2 ± 0.4 (n = 9)	100
HSAcre:Atg5$^{F/F}$:GAA$^{-/-}$	Gastroc	42.6 ± 18.9 (n = 33)	4.1 ± 4.9 (n = 11)	100
	Quad	50.4 ± 14.1 (n = 34)	5.0 ± 4.9 (n = 11)	99
	Heart	148.4 ± 34.5 (n = 14)	0.0 ± 0.0 (n = 11)	100

Each value is the mean ± sd. from the indicated number of animals. The WT levels of glycogen in gastrocnemius/quadriceps are 4.4 ± 4.6 μg glucose/hr/mg protein. *The amount of residual glycogen (minus the WT level) in treated animals was compared to the level of glycogen in the respective tissue of GAA$^{-/-}$ mice.

amount of the hyper-phosphorylated (γ) 4E-BP1 (**Suppl. Fig. 4C**). Furthermore, the mTOR regulation of protein synthesis in GAA$^{-/-}$ muscle does not fit the typical mold. mTOR regulates protein synthesis through the phosphorylation and inactivation of 4E-BP1, a repressor of mRNA translation.[32] In the GAA$^{-/-}$ muscle there is a significant increase in both hypo- (α and β) and hyper-phosphorylated (γ) forms of 4E-BP1 as if conflicting messages are sent for protein synthesis (**Suppl. Fig. 4D**).

The role of FOXO transcription factors, known to be involved in the induction of autophagy,[31] is also not clear in GAA$^{-/-}$ muscle. We have previously shown that FOXO1 was not upregulated in fast muscles of GAA$^{-/-}$ mice.[19] We now demonstrate by real-time PCR that FOXO3 is, in fact, downregulated (~1.5 fold) in fast muscles of GAA$^{-/-}$ mice (n = 5).

Although starvation does not appear to induce autophagy in WT muscle, in GAA$^{-/-}$ muscle we did observe an increase in LC3-II upon starvation (**Suppl. Fig. 4B**). This sensitivity to starvation of fast muscle in the GAA$^{-/-}$ mice may be one of the factors contributing to the increase in autophagy in this disease.

Considering the lack of clarity concerning the classical triggers of autophagy in GAA$^{-/-}$ muscle, we looked at a recently appreciated regulator of autophagy, glycogen synthase kinase 3β (GSK-3β), a protein long known to be involved in glycogen metabolism. A significant decrease in phosphorylation (activation) of GSK-3β is seen in skeletal muscle in both young and old GAA$^{-/-}$ mice (**Fig. 5B and C**) leading to an increase in phosphorylation (inactivation) of glycogen synthase (GS) (**Fig. 5D**). The inactivation of glycogen synthase may reflect a homeostatic adjustment in muscle cells to reduce the cytoplasmic glycogen burden, but it appears to come at a price—the induction of autophagy by activation of GSK-3β, with unfortunate consequences for Pompe skeletal muscle.

To investigate whether or not GSK-3β can induce autophagy in muscle cells, we expressed constitutively active GSK-3β^{S9A} in C2C12 cells. Indeed, immunostaining and western analysis for LC3 showed an induction of autophagy in both C2C12 myoblasts and myotubes (**Fig. 6A and B**). Furthermore, a similar induction of autophagy was observed in GAA$^{-/-}$ derived primary myoblasts,[33] as demonstrated by a two-fold increase of LC3-II/α-tubulin ratio in the cells expressing GSK-3β^{S9A} as compared to those expressing the vector alone (not shown). Consistent with the data in whole muscle, mTOR signaling does not appear to regulate autophagy in C2C12 myotubes, as shown by the absence of changes in the levels of phosphorylated 4E-BP1 in the cells expressing GSK-3β^{S9A} (**Fig. 6D**).

Thus, a homeostatic attempt to downregulate the synthesis of glycogen may contribute to the upregulation of autophagy in this glycogen storage disorder.

Discussion

The autophagic pathway is a critical player in the pathogenesis of Pompe disease and other lysosomal storage diseases, recommending it as a potential site for therapy. This additional therapy is needed because even at very high dosages of the drug the current ERT has a variable effect in skeletal muscle. The rationale for the suppression of autophagy in Pompe skeletal muscle is twofold: first, to prevent the accumulation of a disruptive autophagic buildup in myofibers and second, to reduce the glycogen load.

Muscle-specific suppression of autophagy in Pompe mice reduced glycogen levels in muscle, but the degree of this reduction was significantly different in the MLCcre:Atg7$^{F/F}$:GAA$^{-/-}$ and HSAcre:Atg5$^{F/F}$:GAA$^{-/-}$ strains (with higher glycogen levels in HSAcre:Atg5$^{F/F}$:GAA$^{-/-}$ mice). It is not clear why these two autophagy-deficient strains have different amounts of glycogen. Assuming that autophagy is involved in glycogen trafficking to the lysosomes it appears counterintuitive that muscles from the HSAcre:Atg5$^{F/F}$:GAA$^{-/-}$ in which LC3-II was not present[19] accumulate more glycogen than muscles from the MLCcre:Atg7$^{F/F}$:GAA$^{-/-}$ in which LC3-II is still detectable. One possible explanation is that, in addition to their role in the formation of autophagosomes,[34-38] Atg5 and Atg7 may fulfill other functions in skeletal muscle; for example, it has been recently shown in tumor cells that post-translational cleavage of Atg5 by calpain produces a truncated protein with pro-apoptotic function.[20] Another possibility is that the lack of Atg5 in muscles from HSAcre:Atg5$^{F/F}$:GAA$^{-/-}$ stimulates microautophagy or an Atg5/Atg7-independent alternative autophagy pathway. This

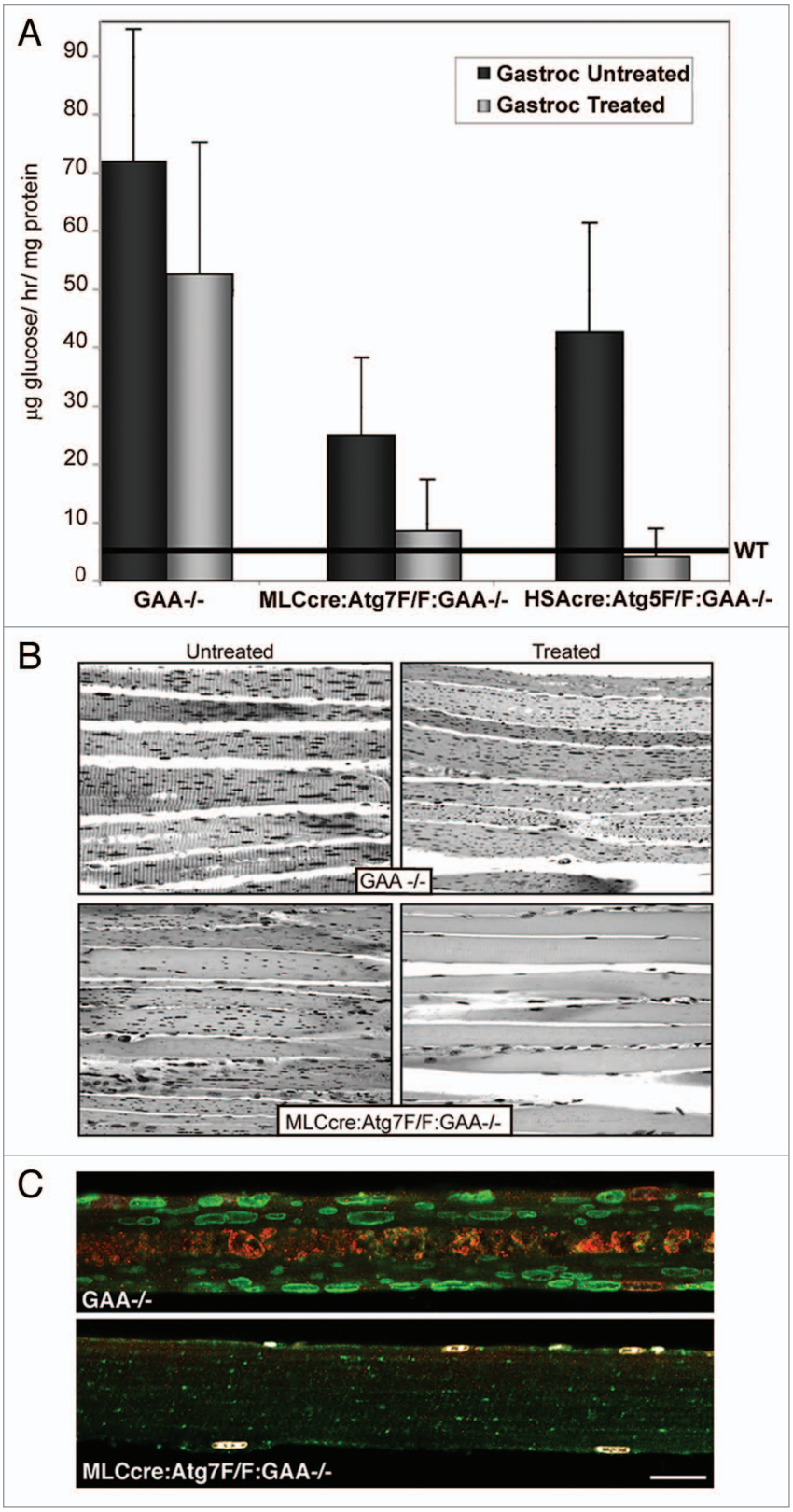

Figure 3. Effect of ERT on glycogen clearance in skeletal muscle of GAA$^{-/-}$ and MLCcre:Atg7$^{F/F}$:GAA$^{-/-}$ mice. (A) Quantitation of glycogen levels in gastrocnemius (fast) muscle from GAA$^{-/-}$, MLCcre:Atg7$^{F/F}$:GAA$^{-/-}$ and HSAcre:Atg5$^{F/F}$:GAA$^{-/-}$ mice before and after ERT (values are mean ± sd.; n = 18–33 for the untreated mice and n = 9–14 for the treated mice). (B) PAS-stained sections (shown in black/white) of gastrocnemius muscle from 4 month-old mice. (C) Immunostaining of single psoas (fast) fibers stained for LAMP-1 (green) and LC3 (red) from 4 month-old ERT-treated GAA$^{-/-}$ and MLCcre:Atg7$^{F/F}$:GAA$^{-/-}$ mice. Comparison of the lower part with that of Figure 1D shows the shrinking of lysosomes after ERT. Bar: 20 microns.

Despite the difference in glycogen levels, both autophagy-deficient Pompe strains responded remarkably well to ERT, suggesting that the removal of autophagic buildup is an important factor that permits this therapy to be so effective. The successful clearance of lysosomal glycogen with rhGAA reported here is unprecedented—it has never been observed in Pompe mice treated with the recombinant enzyme alone.[4,40-43]

The finding in the GAA$^{-/-}$ mice of an increased phosphorylation (inactivation) of glycogen synthase, the enzyme that controls bulk glycogen synthesis, suggests a feedback mechanism used by muscle cells to control the level of cytoplasmic glycogen. The major kinase that phosphorylates GS and reduces its activity is, as indicated by its name, glycogen synthase kinase-3 (GSK-3).[44] The activity of the kinase itself is inhibited by phosphorylation. Glycogen depletion has been observed in skeletal muscle of GSK-3β transgenic mice as well as in muscle cells expressing constitutively active GSK-3β.[45,46] In addition to its role in glycogen metabolism, GSK-3β has been implicated in a large number of pathways and in numerous disorders[47] including lysosomal storage diseases.[48,49] Autophagy has recently joined the long list of pathways affected by the status of GSK-3β. This kinase is a positive regulator of autophagy, as shown by the suppression of autophagy in GSK-3β$^{-/-}$ mouse embryonic fibroblasts (MEFs) as well as in COS-7 cells treated with a GSK-3β inhibitor.[50] A direct correlation between the GSK-3β activity and the induction of autophagy has also been shown in cadmium-treated mouse kidney mesangial cells.[51]

We hypothesize that excess glycogen accumulation in GAA$^{-/-}$ muscle triggers a mechanism by which cytoplasmic glycogen synthesis is suppressed. A relatively slow rate of glycogen accumulation in fast GAA$^{-/-}$ muscle attests to this hypothesis.[40,52] The suppression of glycogen synthesis by activation of GSK-3β may have an unintended consequence in latter, nonconventional autophagy has been recently discovered,[39] and it may transport glycogen to the lysosomes. In the MLCcre:Atg7$^{F/F}$:GAA$^{-/-}$, autophagy is not completely suppressed and therefore, the alternative pathway may not be triggered. This issue, however, is beyond the scope of this paper.

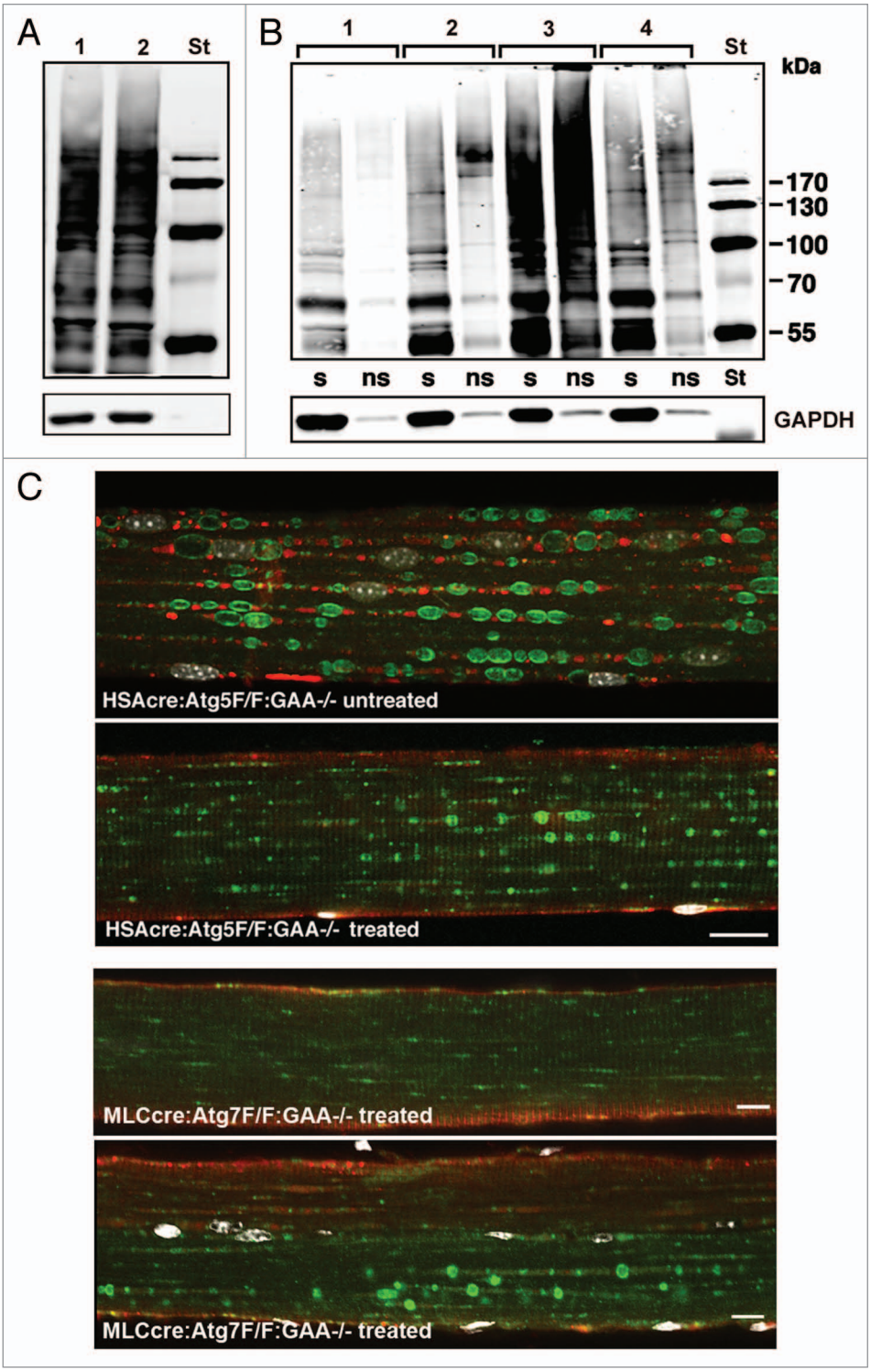

Figure 4. Decrease in the amount of potentially toxic Ub-proteins in muscle from autophagy-deficient GAA$^{-/-}$ strains upon therapy. (A) Western blot of protein lysates from gastrocnemius (fast) muscle with anti-ubiquitin (FK2) antibody. No difference in the levels of Ub-proteins is observed between untreated (lane 1) and ERT-treated (lane 2) GAA$^{-/-}$ mice. (B) Western blot of lysates from gastrocnemius muscle, prepared as detergent (Triton X-100)-soluble (s) and -nonsoluble fractions (ns), with FK2. Lane 1-WT; Lane 2-HSAcre:Atg5$^{F/F}$:WT; Lane 3-HSAcre:Atg5$^{F/F}$:GAA$^{-/-}$ untreated; Lane 4-HSAcre:Atg5$^{F/F}$:GAA$^{-/-}$ treated. Note that there is a modest increase in the amount of Ub-proteins in muscle-specific autophagy-deficient WT mice (lane 2). (C) Single fibers stained for Ub (red) and LAMP-1 (green) show a dramatic decrease in the amount of Ub-proteins upon therapy. Muscle samples were taken from 4-month-old mice. Bars: 20 microns (top two parts); 10 microns (two lower parts). Occasional fibers from autophagy-deficient GAA$^{-/-}$ strains still contain enlarged lysosomes. The distribution of Ub-proteins in untreated fast muscle of MLCcre:Atg7$^{F/F}$:GAA$^{-/-}$ mice (shown in Suppl. Fig. 2) is similar to that in the HSAcre:Atg5$^{F/F}$:GAA$^{-/-}$ mice.

GAA$^{-/-}$ muscle by contributing to the induction of autophagy. This suggests that direct modulation of GS rather than modulation through GSK-3β might be a better therapeutic approach because it can reduce the glycogen load without activation of GSK-3β and thus without induction of autophagy. In fact, the beneficial effect of suppression of glycogen synthesis in skeletal muscle has been recently demonstrated in Pompe mice.[53] Thus, the two different therapeutic approaches, suppression of autophagy or suppression of glycogen synthesis, may have a very similar outcome—lessening the glycogen load and reducing autophagic accumulation.

The potential benefit of combining ERT with suppression of either glycogen synthesis or autophagy depends upon the balance between alleviating the symptoms of Pompe disease by reducing glycogen accumulation and risking the creation of new underlying conditions—a deficiency of glycogen synthase or a deficiency of autophagy in skeletal muscle. The risk of creating glycogen synthase deficiency is discussed in Douillard-Guilloux et al.[53] As for the suppression of autophagy, we and others did not observe any gross phenotypical abnormalities in muscle-specific, autophagy-deficient, wild-type mice.[28,54] However, the impairment of autophagy has been shown to lead to the accumulation of dysfunctional mitochondria and oxidative stress,[54] as well as to muscle atrophy and an age-dependent decrease in force in gastrocnemius muscle.[28] The relatively mild negative effects of inactivation of autophagy that we observe in normal skeletal muscle pale by comparison to the benefits this approach provides in Pompe skeletal muscle. The experiments reported here,

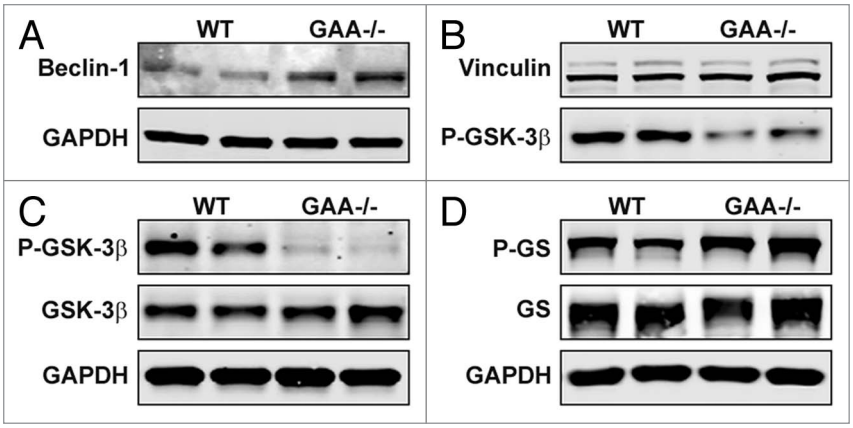

Figure 5. Increase in the levels of Beclin 1 and changes in the phosphorylation status of GSK-3β and glycogen synthase (GS) in muscle from GAA$^{-/-}$ mice. Western blot of protein lysates from gastrocnemius (fast) muscles derived from WT and GAA$^{-/-}$ mice with the indicated antibodies. (A) Upregulation of Beclin 1 indicates that basal autophagy in GAA$^{-/-}$ is induced. (B and C) A markedly decreased phosphorylation (activation) of GSK-3β (on Ser^{9}) is observed in muscle from GAA$^{-/-}$ mice without changes in the amount of total GSK-3β. (D) Increased phosphorylation (inactivation) of GS is shown with anti-phospho-GS antibody (top part) and by an upward shift on the gel with anti-GS antibody. Images shown are representative blots from at least four samples.

we believe, are the first successful attempt to use suppression of autophagy to return cells towards a near normal state.

Bringing the observations reported here to patients with Pompe disease will require developing new approaches that permit a controllable suppression of autophagy directed to skeletal muscle. Oligonucleotides such as shRNA and morpholinos given locally or systemically and pharmaceuticals targeted to the autophagic pathway are sensible ways to consider.

The disturbances of autophagy are involved in the pathogenesis of other lysosomal storage diseases and in other families of diseases and in each, the disturbance is different;[10,14] like Tolstoy's unhappy families, each is unhappy in its own way.[55] Up to the present, however, the approaches to therapy—primarily in neurodegenerative diseases[56] and drug-resistant malignancies[57]—have relied on a limited number of chemicals, established drugs and genes. The promising results so far point to the need for new, more precise and more practical methods of autophagy modulation.

Materials and Methods

Generation and genotyping of muscle-specific autophagy-deficient Pompe mice. Atg7-conditional knockout mice[26] (Atg7 $^{flox/flox}$, referred to as Atg7$^{F/F}$), provided by Dr. Komatsu, were crossed with GAA$^{-/-}$ mice[58] (C57BL/6/129/Sv inbred strain) to produce Atg7$^{F/F}$:GAA$^{-/-}$ mice. We then crossed Atg7$^{F/F}$:GAA$^{-/-}$ mice to a skeletal muscle specific Cre line, which has been generated by homologous recombination of Cre into the *myosin light chain 1f* (MLC) locus (knock-in) (C57BL/6).[59] The Cre mice were generously provided by Dr. Burden (Skirball Institute for Molecular Medicine, New York University Medical center, NY, New York). Cre expression in this line is restricted to fast fibers and is activated early during muscle development. After several rounds of crossing we produced GAA$^{-/-}$ mice deficient for Atg7 specifically in skeletal muscle (MLCcre:Atg7$^{F/F}$:GAA$^{-/-}$).

Genomic DNA was isolated from tail clips using the QuickGene DNA tissue kit (AutoGene, FK-DTS) according to the manufacturer's instructions. The presence of Cre recombinase is indicated by a ~400 bp PCR product made with either primer pair Cre sense/antisense: 5'-CCG GTG AAC GTG CAA AAC AGC CTC TA-3'/5'-CTT CCA GGG CGC GAG TGG ATA GC-3' or 5'-AAG CCC TGA CCC TTT AGA TTC CAT TT-3' (MLC1f promoter)/5'-CCT CAT CAC TCG TTG CAT CGA-3' (anti-sense in Cre). The presence of a wild-type *MLC1f* gene (Cre-negative) is indicated by a ~300 bp PCR product made with MLC1f promoter primer (see above) and an antisense primer in exon 1 of the *MLC1F* gene (5'-GCA GCG GGC TTC TTC ACG TCT TTC T-3'). The *Atg7* wild type, *Atg7$^{F/+}$* and *Atg7$^{F/F}$* alleles were detected with the primer pair 5'-TGG CTG CTA CTT CTG CAA TGA TGT-3'/5'-GAA TAT TCT AAT TCA ACC AGA TCT AGG T-3' (Atg7ex13s/Atg7intr13as) that amplifies a ~1.5 kb fragment from the wt allele and a ~0.35 kb fragment from the floxed allele. The wild-type *Atg7* can also be detected as a PCR fragment of ~0.6 kb with primer pair 5'-GCT GGT TAA AGA CTG TCT AAT AAA GAG CA-3'/5'-CTG CCG CTG AGC CCT GAG AGA GGC CT-3' (intron 13s/mid-intron 13as). The *GAA* wild type, *GAA$^{+/-}$* and *GAA$^{-/-}$* alleles were detected as described.[58] Generation and genotyping of HSAcre:Atg5$^{F/F}$:GAA$^{-/-}$ mice was described previously.[19] In these muscle-specific autophagy-deficient mice, the *Atg5* gene is inactivated in muscle by Cre recombinase driven by the human skeletal actin (HSA) promoter.

The removal of the LoxP-flanked fragment from the *Atg7* gene was confirmed by PCR of genomic DNA with Atg7ex13s primer (5'-TGG CTG CTA CTT CTG CAA TGA TGT-3') and an antisense primer 5'-CAC ACA GAT GTG ACA CTG GAG TGC AGC AT-3' in intron 14. The excision of the loxP-flanked fragment [which includes all the exons starting at exon 14 of the *Atg7* gene[26]] is indicated by the presence of a ~1.2 kb PCR fragment. A combination of three primers—Atg7ex13s/Atg7intr13as/Intron 14as—allows for the detection of both excised (~1.2 kb) and non-excised floxed (~0.4 kb) alleles. Analysis was performed using tail or tissue (muscle or brain) DNA, which was isolated according to the standard procedure. The MLCcre:Atg7$^{F/F}$:GAA$^{-/-}$ colony contained ~150 mice. The clinical signs of muscle disease were monitored in ~ 50 mice.

Enzyme replacement therapy. Two and a half month-old GAA$^{-/-}$, MLCcre:Atg7$^{F/F}$:GAA$^{-/-}$ and HSAcre:Atg5$^{F/F}$:GAA$^{-/-}$ mice received 3 i.v. injections of alglucosidase alfa (provided under a CRADA between the NIH and the Genzyme Corporation) at a dose of 100 mg/kg every other week. Diphenhydramine hydrochloride was injected i.p at a dose of 5 mg/kg 15 minutes before the second and third injections of rhGAA as described.[60]

The mice were sacrificed 5 days after the last injection. Twelve GAA$^{-/-}$, 11 HSAcre:Atg5$^{F/F}$:GAA$^{-/-}$ and 9 MLCcre:Atg7$^{F/F}$:GAA$^{-/-}$ were treated with rhGAA.

Isolation of fixed single muscle fibers and immunofluorescence microscopy. Muscle fixation, isolation of single fibers and immunostaining are described in detail in Raben et al.[12] At least three animals from each genotype were used to obtain single muscle fibers for immunostaining. For each immunostaining and for confocal analysis, at least 20 fibers were isolated from psoas muscle.

Isolation of live single muscle fibers and staining with acridine orange. Single live myofibers were isolated from gastrocnemius muscle. The dissected muscle was placed in a Sylgaard plate containing PBS. Muscles were pinned at resting length and cleaned of any extraneous material under a dissection microscope. Muscles were then digested in 0.2% (w/v) collagenase type 1 (Sigma-Aldrich, C0130-1G) in Dulbecco's modified Eagle's medium (DMEM) (Invitrogen, 11054-020) for 1 h at 37°C in an atmosphere of 5% CO_2. Individual fibers were released under a dissecting microscope by gentle pipeting of partially digested muscle bundles. Individual translucent myofibers (~20 fibers) were plated in each well of a BD cell TAK^{TM}-coated 2-chambered cover glass (BD Pharmingen, 354241) and incubated in plating medium [10% horse serum in DMEM (HyClone Laboratories, SH30074.03)] overnight to let the fibers attach to the surface; the fibers were then incubated with acridine orange (AO) at 2.5 μg/ml for 10 minutes (Molecular Probes, A3568). Fibers were washed three times with medium and then analyzed on a Zeiss 510 confocal microscope (AO emission was collected with a 500–560 nm band pass filter (green) and a 590–660 nm band pass filter (red)).

Western blot. Whole muscle tissues were homogenized in RIPA buffer [PBS containing 1% NP40, 0.5% sodium deoxycholate, 0.1% SDS and a protease inhibitor cocktail tablet (Roche Diagnostics, 11836170001)]. Samples were centrifuged for 30 min at 13,000 rpm at 4°C. Alternatively, detergent-soluble and -insoluble fractions from muscle tissues were obtained as described.[24] Protein concentrations of the supernatants of the total lysates or soluble fractions were measured using the Bio-Rad Protein Assay (Bio-Rad Laboratories, 500-0006). Equal amounts of protein were run on SDS-PAGE gels (Invitrogen, EC6498BOX and EC6078BOX) followed by electro-transfer onto nitrocellulose membranes (Invitrogen, LC2001). Membranes were blocked in 1:1 PBS and Odyssey Blocking Buffer (LI-COR Biosciences, 927-40003), incubated with primary antibodies overnight at 4°C, washed, incubated with secondary antibodies and washed again. Blots were scanned on an infrared imager (LI-COR Biosciences).

The following primary antibodies were used for western blots and immunostaining of fixed fibers: rabbit anti-LC3B (microtubule-associated protein 1 light chain 3) (Sigma, L7543); rat anti-mouse LAMP-1 (Lysosomal-Associated Membrane Protein 1) (BD Pharmingen, 553792); rabbit polyclonal anti-Atg7 (Cell Signaling Technology, 2631); mouse anti-poly-ubiquitinated conjugates (FK2) (BIOMOL International, PW8810); goat polyclonal anti-BECN1 (Beclin 1) (Cell Signaling Technology, 3738); rabbit monoclonal anti-GSK-3β (Cell Signaling Technology, 9315); rabbit monoclonal anti-phospho-GSK-3β (Ser9) (Cell Signaling Technology, 9323); rabbit monoclonal anti-glycogen synthase (Cell Signaling Technology, 3886) and rabbit polyclonal anti-phospho-glycogen synthase (Ser641) (Cell Signaling Technology, 3891); rabbit polyclonal anti-eIF4EBP1 (Abcam,

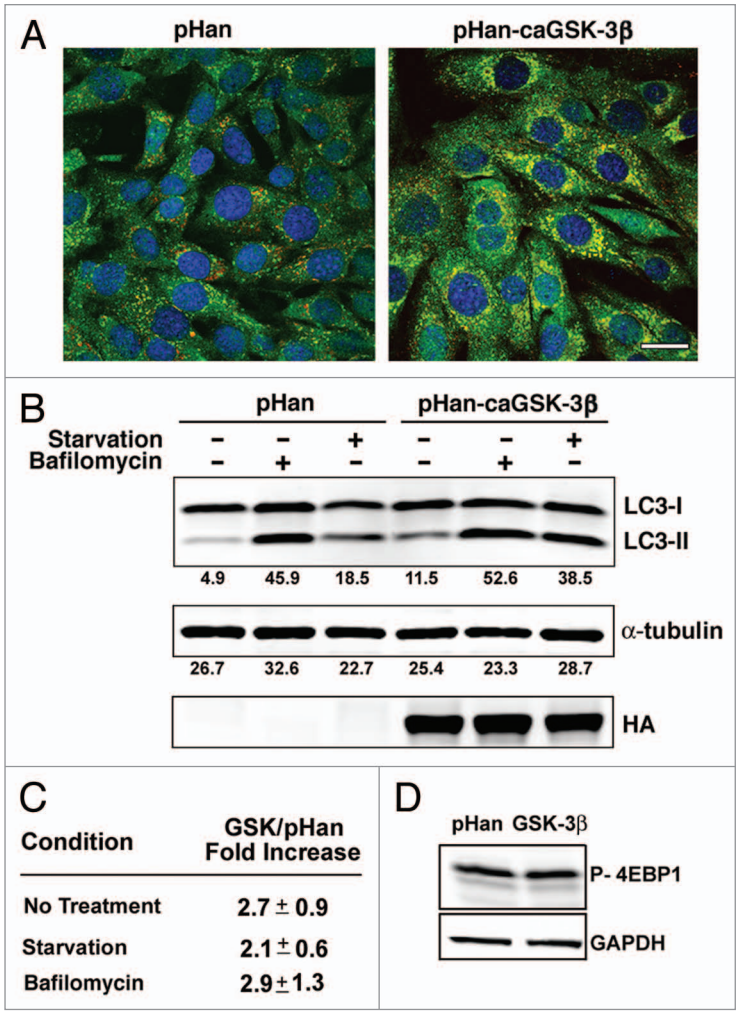

Figure 6. Expression of constitutively active GSK-3β (caGSK-3β) stimulates autophagy in C2C12 cells. (A) Immunostaining of fixed C2C12 myoblasts with LC3 shows an increase in the number of autophagosomes in the cells expressing caGSK-3β (pHan-caGSK-3β) compared to the cells with the vector alone (pHan). The cells were starved in Krebs-Ringer solution for 4 h. (B) Western blot of lysates from myotubes (three-day cultures) expressing caGSK-3β or vector alone with LC3. Myotubes were starved or treated with bafilomycin for 4 h. An increase in the amount of LC3-II is observed under all three conditions in the caGSK-3β cells. The numbers correspond to the densitometry values for LC3-II and α-tubulin (loading control). The expression of hemagglutinin (HA) confirms the expression of caGSK-3β. Images shown are representative blots from at least four experiments. (C) The effect of GSK-3β on autophagy in C2C12 myotubes was assessed as a fold increase of LC3-II/α-tubulin ratio in the cells with or without caGSK-3β. (D) Western blot of lysates from myotubes expressing caGSK-3β or vector alone with antibody against phosphorylated 4E-BP1.

ab2606) and anti-phospho-4E-BP1 (Cell Signaling Technology, 9459); guinea pig polyclonal anti-p62 (ProGen, GP62-N); rabbit polyclonal anti-HA-probe (Santa Cruz Biotechnology, sc-805); mouse monoclonal anti-vinculin (Sigma, V 9131) and mouse monoclonal anti-GAPDH antibody (Abcam, ab9484) served as loading controls. Alexa Fluor-conjugated antibodies (Molecular Probes, A21057, A21076, A21096) were used as secondary antibodies.

Quantitative real-time PCR. Total RNA was extracted from gastrocnemius muscle using TRIzol reagent (Gibco-BRL, 15596-026) according to the standard procedure. The RNA cleanup protocol from the Qiagen RNeasy Mini Kit (Qiagen Sciences, 74104) was used to eliminate short transcripts. 5 μg total RNA was used for cDNA synthesis using the High Capacity cDNA Archive Kit from Applied Biosystems (4368814). The cDNA was then diluted 1:5 and 1 μL of the diluted cDNA was used to perform real-time PCR in 20 μL reactions in 96-well optical plates according to the manufacturer's instructions. SYBR® Green Mouse Foxo3 primer set [SABioscienes, (Mm. 338613)] was use for the analysis. Mouse β-actin was used as an endogenous control.

Electron microscopy. Muscles were fixed and treated as described[12] except that in some cases osmication was done in the presence of 1.5% potassium ferrocyanide ("reduced osmium") for darker glycogen staining.

The source of fast and slow muscles. The white part of gastrocnemius, quadriceps, psoas and extensor digitorum longus (EDL) muscles in mice are a good source of glycolytic fast-twitch type II fibers, whereas soleus muscle is a good source of oxidative slow-twitch type I fibers.[41,61]

Glycogen measurement and light microscopy. Glycogen concentration in skeletal muscle, periodic acid-Schiff (PAS) staining of muscle biopsies and fiber type analysis were performed as described.[19,53,62]

Plasmids, C2C12 cell cultures and transfection. The EcoRI/XhoI fragment containing HA (hemagglutinin)-tagged GSK-3β S^9A was released from the pcDNA3 plasmid (Addgene plasmid #14754). This fragment was then cloned into the EcoRI/SalI sites of the pHan-Puro retroviral expression vector (kindly provided by Dr. M. Fulco, NIAMS, NIH). GSK-3β S^9A is a glycogen synthase kinase in which serine 9 of human GSK-3β is mutated to alanine. When expressed, the mutant kinase is constitutively active (ca). The pHan-Puro-GFP vector was used as a control. Culturing and transfection of C2C12 myoblasts and myotubes were done according to the standard procedures with some modifications. Viral supernatants were obtained by transfection of Phoenix cells (Orbigen, RVC-10002) with the retroviral expression vectors (pHan-Puro or pHan-Puro containing constitutively active GSK-3βS9A) using the calcium phosphate method. C2C12 mouse myoblasts were grown in DMEM supplemented with 20% fetal bovine serum (Atlanta Biologicals, S11550), 0.5% chick embryo extract (Sera Laboratories International Ltd., CE-650-T) and 1% penicillin-streptomycin-glutamine (Invitrogen, 10378-016). The cells were seeded into 6-well plates (3×10^4 cells/well) and infected with the filtered viral supernatant containing 8 μg/ml Polybrene (Sigma, H9268-5G). The plates were centrifuged at 3,700 rpm at room temperature for 1.5 h, placed at 37°C overnight, and then selected in the presence of 2 μg/ml of puromycin (Invitrogen, A1113803). For differentiation of C2C12 cells into myotubes, the cells were grown to near confluence and the culture medium was changed to DMEM containing 1% penicillin-streptomycin-glutamine and 5% horse serum (HyClone Laboratories, SH30074.03).

For starvation, the cells (myoblasts or myotubes) were incubated in Krebs-Ringer solution at 37°C for 4 h. Alternatively, cells were treated with 400 nM bafilomycin [(Sigma, 131793) in DMEM containing serum and supplements to inhibit autophagosome-lysosome fusion[63]]. For western analysis the cells were lysed in RIPA buffer with inhibitors. For immunostaining, the cells were fixed with 2% paraformaldehyde (Electron Microscopy Sciences, 15710) in 0.1 M phosphate buffer for 1 h. After several washes with PBS, myoblasts were incubated with blocking reagent (MOM kit; Vector Laboratories, BMK-2202) for 1 h at room temperature; the cells were then incubated with primary antibodies overnight at 4°C, washed with PBS, incubated with secondary antibody for 2 h and washed again with PBS before examination by confocal microscopy (Zeiss LSM 510).

Force measurements. Force measurements on the EDL (extensor digitorum longus) muscles were conducted as described.[64] Force measurements on single fibers isolated from psoas muscle were done as described.[65] The overall muscle strength was evaluated by grip strength measurements using a grip-strength meter (Columbus Instruments, 1027MPB); the data were normalized by body weight and expressed as KGF/kg as described.[66]

Animal care and experiments were conducted in accordance with the National Institutes of Health Guide for the Care and Use of Laboratory Animals.

Acknowledgements

We would like to thank Dr. John O'Shea and Dr. Rosa Puertollano for their helpful comments. We are also grateful to Dr. Marcella Fulco and Dr. Kristien Zaal (NIAMS, NIH) for helping with cell cultures and transfections. We would also like to thank Dr. J.H. Tao-Cheng (NINDS, NIH) for help with the EM.

Financial Support

This research was supported by the Intramural Research Program of the NIAMS of the NIH. Dr. Takikita was supported in part by a CRADA between the NIH and Genzyme Corporation.

Note

Supplementary materials can be found at:
www.landesbioscience.com/supplement/RabenAUTO6-8-Sup.pdf
www.landesbioscience.com/supplement/RabenAUTO6-8-SupVid01.mpg
www.landesbioscience.com/supplement/RabenAUTO6-8-SupVid02.mpg

References

1. Hirschhorn R, Reuser AJ. Glycogen Storage Disease Type II: Acid alpha-Glucosidase (Acid Maltase) Deficiency. The Metabolic and Molecular Basis of Inherited Disease. McGraw-Hill 2001; 3389-420.
2. Kishnani PS, Howell RR. Pompe disease in infants and children. J Pediatr 2004; 144:35-43.
3. Hagemans ML, Winkel LP, Hop WC, Reuser AJ, Van Doorn PA, Van der Ploeg AT. Disease severity in children and adults with Pompe disease related to age and disease duration. Neurology 2005; 64:2139-41.
4. Raben N, Jatkar T, Lee A, Lu N, Dwivedi S, Nagaraju K, et al. Glycogen stored in skeletal but not in cardiac muscle in acid alpha-glucosidase mutant (Pompe) mice is highly resistant to transgene-encoded human enzyme. Mol Ther 2002; 6:601-8.
5. Kishnani PS, Corzo D, Nicolino M, Byrne B, Mandel H, Hwu WL, et al. Recombinant human acid [alpha]-glucosidase: major clinical benefits in infantile-onset Pompe disease. Neurology 2007; 68:99-109.
6. Nicolino M, Byrne B, Wraith JE, Leslie N, Mandel H, Freyer DR, et al. Clinical outcomes after long-term treatment with alglucosidase alfa in infants and children with advanced Pompe disease. Genet Med 2009; 11:210-9.
7. Fukuda T, Ahearn M, Roberts A, Mattaliano RJ, Zaal K, Ralston E, et al. Autophagy and mistargeting of therapeutic enzyme in skeletal muscle in pompe disease. Mol Ther 2006; 14:831-9.
8. Raben N, Takikita S, Pittis MG, Bembi B, Marie SKN, Roberts A, et al. Deconstructing Pompe disease by analyzing single muscle fibers. Autophagy 2007; 3:546-52.
9. He C, Klionsky DJ. Regulation mechanisms and signaling pathways of autophagy. Annu Rev Genet 2009; 43:67-93.
10. Mizushima N, Levine B, Cuervo AM, Klionsky DJ. Autophagy fights disease through cellular self-digestion. Nature 2008; 451:1069-75.
11. Komatsu M, Ueno T, Waguri S, Uchiyama Y, Kominami E, Tanaka K. Constitutive autophagy: vital role in clearance of unfavorable proteins in neurons. Cell Death Differ 2007; 14:887-94.
12. Raben N, Shea L, Hill V, Plotz P. Monitoring autophagy in lysosomal storage disorders. Methods Enzymol 2009; 453:417-49.
13. Ballabio A, Gieselmann V. Lysosomal disorders: from storage to cellular damage. Biochim Biophys Acta 2009; 1793:684-96.
14. Levine B, Kroemer G. Autophagy in the pathogenesis of disease. Cell 2008; 132:27-42.
15. Rubinsztein DC, Gestwicki JE, Murphy LO, Klionsky DJ. Potential therapeutic applications of autophagy. Nat Rev Drug Discov 2007; 6:304-12.
16. Brech A, Ahlquist T, Lothe RA, Stenmark H. Autophagy in tumour suppression and promotion. Mol Oncol 2009; 3:366-75.
17. Schiaffino S, Hanzlikova V. Autophagic degradation of glycogen in skeletal muscles of the newborn rat. J Cell Biol 1972; 52:41-51.
18. Kotoulas OB, Kalamidas SA, Kondomerkos DJ. Glycogen autophagy in glucose homeostasis. Pathol Res Pract 2006; 202:631-8.
19. Raben N, Hill V, Shea L, Takikita S, Baum R, Mizushima N, et al. Suppression of autophagy in skeletal muscle uncovers the accumulation of ubiquitinated proteins and their potential role in muscle damage in Pompe disease. Hum Mol Genet 2008; 17:3897-908.
20. Yousefi S, Perozzo R, Schmid I, Ziemiecki A, Schaffner T, Scapozza L, et al. Calpain-mediated cleavage of Atg5 switches autophagy to apoptosis. Nat Cell Biol 2006; 8:1124-32.
21. Raben N, Nagaraju K, Lee E, Plotz P. Modulation of disease severity in mice with targeted disruption of the acid alpha-glucosidase gene. Neuromuscul Disord 2000; 10:283-91.
22. Bonifacino JS, Traub LM. Signals for sorting of transmembrane proteins to endosomes and lysosomes. Annu Rev Biochem 2003; 72:395-447.
23. Ciechanover A. Proteolysis: from the lysosome to ubiquitin and the proteasome. Nat Rev Mol Cell Biol 2005; 6:79-87.
24. Hara T, Nakamura K, Matsui M, Yamamoto A, Nakahara Y, Suzuki-Migishima R, et al. Suppression of basal autophagy in neural cells causes neurodegenerative disease in mice. Nature 2006; 441:885-9.
25. Komatsu M, Waguri S, Chiba T, Murata S, Iwata J, Tanida I, et al. Loss of autophagy in the central nervous system causes neurodegeneration in mice. Nature 2006; 441:880-4.
26. Komatsu M, Waguri S, Ueno T, Iwata J, Murata S, Tanida I, et al. Impairment of starvation-induced and constitutive autophagy in Atg7-deficient mice. J Cell Biol 2005; 169:425-34.
27. Bifsha P, Landry K, Ashmarina L, Durand S, Seyrantepe V, Trudel S, et al. Altered gene expression in cells from patients with lysosomal storage disorders suggests impairment of the ubiquitin pathway. Cell Death Differ 2007; 14:511-23.
28. Masiero E, Agatea L, Mammucari C, Blaauw B, Loro E, Komatsu M, et al. Autophagy is required to maintain muscle mass. Cell Metab 2009; 10:507-15.
29. Cao Y, Klionsky DJ. Physiological functions of Atg6/Beclin 1: a unique autophagy-related protein. Cell Res 2007; 17:839-49.
30. Mizushima N, Yamamoto A, Matsui M, Yoshimori T, Ohsumi Y. In vivo analysis of autophagy in response to nutrient starvation using transgenic mice expressing a fluorescent autophagosome marker. Mol Biol Cell 2004; 15:1101-11.
31. Mammucari C, Milan G, Romanello V, Masiero E, Rudolf R, Del Piccolo P, et al. FoxO3 controls autophagy in skeletal muscle in vivo. Cell Metab 2007; 6:458-71.
32. Hay N, Sonenberg N. Upstream and downstream of mTOR. Genes Dev 2004; 18:1926-45.
33. Takikita S, Myerowitz R, Zaal K, Raben N, Plotz PH. Murine muscle cell models for Pompe disease and their use in studying therapeutic approaches. Mol Genet Metab 2009; 96:208-17.
34. Kabeya Y, Mizushima N, Ueno T, Yamamoto A, Kirisako T, Noda T, et al. LC3, a mammalian homologue of yeast Apg8p, is localized in autophagosome membranes after processing. EMBO J 2000; 19:5720-8.
35. Mizushima N, Ohsumi Y, Yoshimori T. Autophagosome formation in mammalian cells. Cell Struct Funct 2002; 27:421-9.
36. Kabeya Y, Mizushima N, Yamamoto A, Oshitani-Okamoto S, Ohsumi Y, Yoshimori T. LC3, GABARAP and GATE16 localize to autophagosomal membrane depending on form-II formation. J Cell Sci 2004; 117:2805-12.
37. Tanida I, Ueno T, Kominami E. LC3 conjugation system in mammalian autophagy. Int J Biochem Cell Biol 2004; 36:2503-18.
38. Ohsumi Y. Molecular dissection of autophagy: two ubiquitin-like systems. Nat Rev Mol Cell Biol 2001; 2:211-6.
39. Nishida Y, Arakawa S, Fujitani K, Yamaguchi H, Mizuta T, Kanaseki T, et al. Discovery of Atg5/Atg7-independent alternative macroautophagy. Nature 2009; 461:654-8.
40. Raben N, Danon M, Gilbert AL, Dwivedi S, Collins B, Thurberg BL, et al. Enzyme replacement therapy in the mouse model of Pompe disease. Mol Genet Metab 2003; 80:159-69.
41. Hawes ML, Kennedy W, O'Callaghan MW, Thurberg BL. Differential muscular glycogen clearance after enzyme replacement therapy in a mouse model of Pompe disease. Mol Genet Metab 2007; 91:343-51.
42. McVie-Wylie AJ, Lee KL, Qiu H, Jin X, Do H, Gotschall R, et al. Biochemical and pharmacological characterization of different recombinant acid alpha-glucosidase preparations evaluated for the treatment of Pompe disease. Mol Genet Metab 2008; 94:448-55.
43. Zhu Y, Jiang JL, Gumlaw NK, Zhang J, Bercury SD, Ziegler RJ, et al. Glycoengineered acid alpha-glucosidase with improved efficacy at correcting the metabolic aberrations and motor function deficits in a mouse model of Pompe disease. Mol Ther 2009; 17:954-63.
44. Hemmings BA, Yellowlees D, Kernohan JC, Cohen P. Purification of glycogen synthase kinase 3 from rabbit skeletal muscle. Copurification with the activating factor (FA) of the (Mg-ATP) dependent protein phosphatase. Eur J Biochem 1981; 119:443-51.
45. Pearce NJ, Arch JR, Clapham JC, Coghlan MP, Corcoran SL, Lister CA, et al. Development of glucose intolerance in male transgenic mice overexpressing human glycogen synthase kinase-3beta on a muscle-specific promoter. Metabolism 2004; 53:1322-30.
46. MacAulay K, Blair AS, Hajduch E, Terashima T, Baba O, Sutherland C, et al. Constitutive activation of GSK3 downregulates glycogen synthase abundance and glycogen deposition in rat skeletal muscle cells. J Biol Chem 2005; 280:9509-18.
47. Kockeritz L, Doble B, Patel S, Woodgett JR. Glycogen synthase kinase-3—an overview of an over-achieving protein kinase. Curr Drug Targets 2006; 7:1377-88.
48. Walls KC, Klocke BJ, Saftig P, Shibata M, Uchiyama Y, Roth KA, et al. Altered regulation of phosphatidylinositol 3-kinase signaling in cathepsin D-deficient brain. Autophagy 2007; 3:222-9.
49. Bi X, Liu J, Yao Y, Baudry M, Lynch G. Deregulation of the phosphatidylinositol-3 kinase signaling cascade is associated with neurodegeneration in Npc1$^{-/-}$ mouse brain. Am J Pathol 2005; 167:1081-92.
50. Sarkar S, Krishna G, Imarisio S, Saiki S, O'Kane CJ, Rubinsztein DC. A rational mechanism for combination treatment of Huntington's disease using lithium and rapamycin. Hum Mol Genet 2008; 17:170-8.
51. Wang SH, Shih YL, Kuo TC, Ko WC, Shih CM. Cadmium toxicity toward autophagy through ROS-activated GSK-3beta in mesangial cells. Toxicol Sci 2009; 108:124-31.
52. Raben N, Fukuda T, Gilbert AL, de Jong D, Thurberg BL, Mattaliano RJ, et al. Replacing acid alpha-glucosidase in Pompe disease: recombinant and transgenic enzymes are equipotent, but neither completely clears glycogen from type II muscle fibers. Mol Ther 2005; 11:48-56.
53. Douillard-Guilloux G, Raben N, Takikita S, Ferry A, Vignaud A, Guillet-Deniau I, et al. Restoration of muscle functionality by genetic suppression of glycogen synthesis in a murine model of Pompe disease. Hum Mol Genet 2009.
54. Wu JJ, Quijano C, Chen E, Liu H, Cao L, Fergusson MM, et al. Mitochondrial dysfunction and oxidative stress mediate the physiological impairment induced by the disruption of autophagy. Aging (Albany NY) 2009; 1:425-37.
55. Leo Tolstoy. Anna Karenina (Penguin Book: New York, 2000) p.1.
56. Rami A. Review: Autophagy in neurodegeneration: firefighter and/or incendiarist? Neuropathol Appl Neurobiol 2009; 35:449-61.
57. Amaravadi RK, Yu D, Lum JJ, Bui T, Christophorou MA, Evan GI, et al. Autophagy inhibition enhances therapy-induced apoptosis in a Myc-induced model of lymphoma. J Clin Invest 2007; 117:326-36.
58. Raben N, Nagaraju K, Lee E, Kessler P, Byrne B, Lee L, et al. Targeted disruption of the acid alpha-glucosidase gene in mice causes an illness with critical features of both infantile and adult human glycogen storage disease type II. J Biol Chem 1998; 273:19086-92.
59. Bothe GW, Haspel JA, Smith CL, Wiener HH, Burden SJ. Selective expression of Cre recombinase in skeletal muscle fibers. Genesis 2000; 26:165-6.

60. Zhu Y, Li X, McVie-Wylie A, Jiang C, Thurberg BL, Raben N, et al. Carbohydrate-remodeled acid alpha-glucosidase with higher affinity for the cation-independent mannose 6-phosphate receptor demonstrates improved delivery to muscles of Pompe mice. Biochem J 2005; 389(Pt 3):619-28.
61. Burkholder TJ, Fingado B, Baron S, Lieber RL. Relationship between muscle fiber types and sizes and muscle architectural properties in the mouse hindlimb. J Morphol 1994; 221:177-90.
62. Ogilvie RW, Feeback DL. A metachromatic dye-ATPase method for the simultaneous identification of skeletal muscle fiber types I, IIA, IIB and IIC. Stain Technol 1990; 65:231-41.
63. Yamamoto A, Tagawa Y, Yoshimori T, Moriyama Y, Masaki R, Tashiro Y. Bafilomycin A1 prevents maturation of autophagic vacuoles by inhibiting fusion between autophagosomes and lysosomes in rat hepatoma cell line, H-4-II-E cells. Cell Struct Funct 1998; 23:33-42.
64. Brooks SV, Faulkner JA. Contractile properties of skeletal muscles from young, adult and aged mice. J Physiol 1988; 404:71-82.
65. Xu S, Galperin M, Melvin G, Horowits R, Raben N, Plotz P, et al. Impaired organization and function of myofilaments in single muscle fibers from a mouse model of Pompe disease. J Appl Physiol 2010; 108:1383-8.
66. Spurney CF, Gordish-Dressman H, Guerron AD, Sali A, Pandey GS, Rawat R, et al. Preclinical drug trials in the mdx mouse: Assessment of reliable and sensitive outcome measures. Muscle Nerve 2009; 39:591-602.